

Activity Detection in Distributed MIMO: Distributed AMP via Likelihood Ratio Fusion

Jianan Bai and Erik G. Larsson

Abstract—We develop a new algorithm for activity detection for grant-free multiple access in distributed multiple-input multiple-output (MIMO). The algorithm is a distributed version of the approximate message passing (AMP) based on a soft combination of likelihood ratios computed independently at multiple access points. The underpinning theoretical basis of our algorithm is a new observation that we made about the state evolution in the AMP. Specifically, with a minimum mean-square error denoiser, the state maintains a block-diagonal structure whenever the covariance matrices of the signals have such a structure. We show by numerical examples that the algorithm outperforms competing schemes from the literature.

Index Terms—Distributed AMP, activity detection, distributed MIMO.

I. INTRODUCTION

LIMITLESS connectivity is envisioned to be one of the key features in next-generation wireless networks. Distributed multiple-input multiple-output (MIMO), also known as cell-free massive MIMO, is a promising technology to achieve this goal [1]. To support massive connectivity and low latency, grant-free multiple access (GFMA) has been proposed to reduce signaling compared to grant-based access.

In GFMA, an access point (AP) needs to identify the active users and estimate their channels based on received pilots. Due to the massive number of devices and the limited coherence block size, assigning mutually orthogonal pilot sequences to all devices becomes impractical. The resulting non-orthogonality of the pilots makes the problem of joint activity detection and channel estimation (JADCE) challenging. In typical application scenarios, devices only sporadically access the network. This enables JADCE in GFMA to be cast as a compressed sensing (CS) problem [2].

For co-located MIMO, GFMA with JADCE has been extensively studied. Specifically, the approximate message passing (AMP) [3], a low-complexity iterative algorithm for CS, has been successfully used [2], [4]. An alternative approach is to make a prior assumption on the fading statistics (typically Rayleigh) and find the maximum-likelihood estimates of the signal strengths, using, for example, coordinate descent [5]. This approach, called “covariance-based” in [5] and herein, outperforms AMP for activity detection in co-located MIMO when the number of antennas is large.

The authors are with the Department of Electrical Engineering (ISY), Linköping University, 58183 Linköping, Sweden (email: jianan.bai@liu.se, erik.g.larsson@liu.se). This work was supported in part by ELLIIT, the KAW foundation, and the European Union’s Horizon 2020 research and innovation program under grant agreement no. 101013425 (REINDEER). The computations were enabled by resources provided by the Swedish National Infrastructure for Computing (SNIC), partially funded by the Swedish Research Council through grant agreement no. 2018-05973.

For distributed MIMO, several algorithms also exist. In particular, the AMP can be applied with an assumption of spatially correlated channels with a block-diagonal covariance that reflects that the APs are geographically distributed [6]. Extensions of the covariance-based approach to distributed MIMO are also possible, although not uncomplicated. A naive implementation requires solving polynomial equations whose order is proportional to the number of APs. In [7], the authors proposed a covariance-based approach with clustering to effectively combine signals from only a subset of APs. Eventually, however, all these approaches [6], [7] require all APs to send their received pilot signals to a central processing unit (CPU) and thus incur a high fronthaul load; additionally, they require fully centralized processing of the signals.

We are only aware of one existing paper that attempts to construct a distributed implementation of the AMP for JADCE in GFMA in distributed MIMO: [8]. This paper proposed to let each AP run the AMP algorithm to make hard decisions on device activities and then send these decisions to a CPU for fusion. There are also distributed versions of the AMP, developed for more general use cases: [9] proposed an iterative solution that requires a two-round communication between the computing nodes and the central node (APs and CPU in our application) and [10] that applied a consensus propagation protocol. These algorithms, however, are inapplicable to GFMA.

Technical contribution: We develop a distributed version of AMP and apply it to JADCE for GFMA in distributed MIMO. By examining the AMP state evolution, we show that when the channels are uncorrelated across different APs, the log-likelihood ratio (LLR) of the device activity is equal to the sum of local LLRs obtained per AP. This enables each AP to compute a local LLR and send it for soft decision fusion. Our algorithm performs closely to the nominal centralized AMP, and it yields the channel estimates as a byproduct.

II. SYSTEM MODEL AND POWER ALLOCATION

We consider the uplink of a distributed MIMO system, where K APs jointly serve N single-antenna devices. Each AP has M receive antennas, and the total number of antennas in the system is denoted by $M_{\text{tot}} = KM$. Each device, $n \in \mathcal{N}$, is pre-allocated a pilot sequence $\phi_n = [\phi_{1n}, \dots, \phi_{Ln}]^T \in \mathbb{C}^L$ with unit energy, i.e., $\|\phi_n\|^2 = 1$. In each time slot, the activity of device n is modeled by a binary random variable, $a_n \sim \text{Bernoulli}(\epsilon_n)$.

The received signal, $\mathbf{Y}_k \in \mathbb{C}^{L \times M}$, at the k -th AP can be expressed as

$$\mathbf{Y}_k = \sum_{n \in \mathcal{N}} \sqrt{L p_n} a_n \phi_n \tilde{\mathbf{h}}_{kn}^T + \mathbf{W}_k, \quad (1)$$

where $p_n \in [0, p_{\max}]$ is the transmit power of device n . The channel between AP k and device n is modeled by $\tilde{\mathbf{h}}_{kn} \sim \mathcal{CN}(\mathbf{0}, \tilde{\mathbf{R}}_{kn})$, where $\tilde{\mathbf{R}}_{kn} \in \mathbb{C}^{M \times M}$ is the spatial correlation matrix, and $\beta_{kn} = \text{tr}(\tilde{\mathbf{R}}_{kn})/M$ can be interpreted as the large-scale fading coefficient (LSFC). The channel is assumed to be uncorrelated between different APs and devices. The noise matrix $\mathbf{W}_k \in \mathbb{C}^{L \times M}$ has i.i.d. entries with $\mathcal{CN}(0, \sigma^2)$ elements, where σ^2 is the noise variance.

For brevity of notation, we define the effective channel $\mathbf{h}_{kn} \triangleq \sqrt{L p_n} \tilde{\mathbf{h}}_{kn}$, which has the distribution $\mathcal{CN}(\mathbf{0}, \mathbf{R}_{kn})$, where $\mathbf{R}_{kn} = L p_n \tilde{\mathbf{R}}_{kn}$, and $\rho_{kn} = L p_n \beta_{kn}$ can be interpreted as the received signal strength of device n at AP k .

Denoting the pilot matrix by $\Phi = [\phi_1, \dots, \phi_N]$, the effective channel matrix by $\mathbf{H}_k = [\mathbf{h}_{k1}, \dots, \mathbf{h}_{kn}]^T$, and the vector of device activities by $\mathbf{a} = [a_1, \dots, a_N]^T$, the received signal model in (1) can be written as

$$\mathbf{Y}_k = \Phi \mathbf{D}_a \mathbf{H}_k + \mathbf{W}_k. \quad (2)$$

By combining the received signal at all APs, we obtain

$$\mathbf{Y} = \Phi \mathbf{D}_a \underbrace{[\mathbf{H}_1, \dots, \mathbf{H}_K]}_{\triangleq \mathbf{H}} + \underbrace{[\mathbf{W}_1, \dots, \mathbf{W}_K]}_{\triangleq \mathbf{W}}, \quad (3)$$

where $\mathbf{H} = [\mathbf{h}_1, \dots, \mathbf{h}_N]^T$ and $\mathbf{h}_n = [\mathbf{h}_{1n}^T, \dots, \mathbf{h}_{Kn}^T]^T$ is the channel from device n to all APs. Note that by assuming uncorrelated fading across different APs, \mathbf{h}_n has the distribution $\mathcal{CN}(\mathbf{0}, \mathbf{R}_n)$, where \mathbf{R}_n is block-diagonal: $\mathbf{R}_n = \text{bdiag}(\mathbf{R}_{1n}, \dots, \mathbf{R}_{Kn})$.

A. Power Allocation

In distributed MIMO, since the APs are spread out, the channel gains from a device to different APs vary significantly. The signal strength from a device is generally larger at APs that are physically close to the device than at other APs.

We propose a user-centric power allocation scheme that comes in a few different variations. The details are as follows:

- 1) Each device n is associated with the subset of APs, say \mathcal{K}_n^p , for which the LSFCs exceed a threshold β_n^{th} :

$$\mathcal{K}_n^p = \{k \in \mathcal{K} : \beta_{kn} > \beta_n^{\text{th}}\}. \quad (4)$$

If no AP satisfies this requirement, we associate the device to the AP with the largest LSFC, i.e.,

$$\bar{\mathcal{K}}_n^p = \mathcal{K}_n^p \cup \{\arg \max_{k \in \mathcal{K}} \beta_{kn}\}. \quad (5)$$

- 2) For each device, a coefficient s_n is calculated. We consider the three different choices:

$$s_n = \begin{cases} 1, & \text{FullPower} \\ \max_{k \in \bar{\mathcal{K}}_n^p} \beta_{kn}, & \text{MasterAP} \\ \frac{1}{|\bar{\mathcal{K}}_n^p|} \sum_{k \in \bar{\mathcal{K}}_n^p} \beta_{kn}, & \text{AvgAP} \end{cases}. \quad (6)$$

- 3) For each device, the transmit power is set to

$$p_n = \min \{s_{\min}/s_n, 1\} p_{\max}, \quad (7)$$

where $s_{\min} = \min_{n': |\mathcal{K}_{n'}^p| \geq 1} s_{n'}$ is the minimum coefficient among all devices for which at least one AP satisfies the LSFC requirement, i.e., $\beta_{kn} > \beta_n^{\text{th}}$.

III. ACTIVITY DETECTION IN DISTRIBUTED MIMO

The system model in (3) is an instance of the linear measurement model $\mathbf{Y} = \Phi \mathbf{X} + \mathbf{W}$, where the unknown signal matrix \mathbf{X} is row sparse, and each row $\mathbf{x}_n^T = a_n \mathbf{h}_n^T$ has a Bernoulli-Gaussian distribution. Therefore, the activity detection becomes a support recovery problem in CS, which can be solved using the AMP algorithm.

A. AMP with MMSE Denoiser and Likelihood-Ratio Test

By initializing $\mathbf{Z}^0 = \mathbf{Y}$ and $\hat{\mathbf{X}}^0 = \mathbf{0}_{N \times M_{\text{tot}}}$, the AMP iteration $t \in \{0, 1, \dots\}$ for complex-valued signals is [2],

$$\hat{\mathbf{x}}_n^{t+1} = \mathbf{g}_t \left(\underbrace{(\mathbf{Z}^t)^T \phi_n^* + \hat{\mathbf{x}}_n^t}_{\triangleq \boldsymbol{\xi}_n^t} \right), \quad \forall n \in \mathcal{N}, \quad (8)$$

$$\mathbf{Z}^{t+1} = \mathbf{Y} - \Phi \hat{\mathbf{X}}^{t+1} + \frac{1}{L} \mathbf{Z}^t \sum_{n \in \mathcal{N}} \mathbf{g}'_t(\boldsymbol{\xi}_n^t), \quad (9)$$

where $\hat{\mathbf{X}}^t = [\hat{\mathbf{x}}_1^t, \dots, \hat{\mathbf{x}}_N^t]^T$. Here, $\mathbf{g}_t(\cdot) : \mathbb{C}^{M_{\text{tot}}} \rightarrow \mathbb{C}^{M_{\text{tot}}}$ is the denoiser and $\mathbf{g}'_t(\boldsymbol{\xi})$ represents its Jacobian at $\boldsymbol{\xi}$.

As demonstrated in the state evolution analysis [3], under some mild conditions and in the large-system limit, $\boldsymbol{\xi}_n^t$ behaves like a Gaussian-noise corrupted version of \mathbf{x}_n , i.e.,

$$\boldsymbol{\xi}_n^t \sim \mathbf{x}_n + \mathcal{CN}(\mathbf{0}, \boldsymbol{\Sigma}^t). \quad (10)$$

In (10), $\boldsymbol{\Sigma}^t$ is referred to as the *state*; this state evolves by

$$\boldsymbol{\Sigma}^{t+1} = \sigma^2 \mathbf{I} + \frac{1}{L} \sum_{n \in \mathcal{N}} \mathbb{E} \left[(\mathbf{g}_t(\mathbf{x}_n + \mathbf{v}^t) - \mathbf{x}_n) (\mathbf{g}_t(\mathbf{x}_n + \mathbf{v}^t) - \mathbf{x}_n)^H \right], \quad (11)$$

where \mathbf{v}^t has distribution $\mathcal{CN}(\mathbf{0}, \boldsymbol{\Sigma}^t)$ and is independent of \mathbf{x}_n , and the expectation is taken over the joint distribution of \mathbf{x}_n and \mathbf{v}^t . The initial state is given by

$$\boldsymbol{\Sigma}^0 = \sigma^2 \mathbf{I} + \frac{1}{L} \sum_{n \in \mathcal{N}} \mathbf{R}_n. \quad (12)$$

The minimum mean-square error (MMSE) denoiser is given by the MMSE estimate of \mathbf{x}_n given $\boldsymbol{\xi}_n^t$,

$$\mathbf{g}_t(\boldsymbol{\xi}_n^t) = \mathbb{E}[\mathbf{x}_n | \boldsymbol{\xi}_n^t] = \theta_n^t(\boldsymbol{\xi}_n^t) \cdot \boldsymbol{\Psi}_n^t \boldsymbol{\xi}_n^t, \quad (13)$$

where

$$\theta_n^t(\boldsymbol{\xi}) = \left(1 + \frac{1 - \epsilon_n}{\epsilon_n} \frac{|\mathbf{R}_n + \boldsymbol{\Sigma}^t|}{|\boldsymbol{\Sigma}^t|} \exp(-\boldsymbol{\xi}^H \boldsymbol{\Omega}_n^t \boldsymbol{\xi}) \right)^{-1}, \quad (14)$$

$$\boldsymbol{\Psi}_n^t = \mathbf{R}_n (\mathbf{R}_n + \boldsymbol{\Sigma}^t)^{-1}, \quad (15)$$

$$\boldsymbol{\Omega}_n^t = (\boldsymbol{\Sigma}^t)^{-1} - (\mathbf{R}_n + \boldsymbol{\Sigma}^t)^{-1}. \quad (16)$$

The support recovery problem is equivalent to the detection of the non-zero entries in the binary vector \mathbf{a} . To determine the value of a_n , we consider the binary hypothesis test

$$\mathcal{H}_0 : a_n = 0 \quad \text{and} \quad \mathcal{H}_1 : a_n = 1. \quad (17)$$

The likelihood-ratio test (LRT) is given by¹

$$\ell_n \triangleq \frac{p(\boldsymbol{\xi}_n | a_n = 0)}{p(\boldsymbol{\xi}_n | a_n = 1)} \stackrel{\mathcal{H}_0}{\geq} \gamma, \quad (18)$$

¹For brevity, we henceforth omit the iteration index t in the superscripts.

where $\gamma > 0$ is the decision threshold. According to (10), the likelihood-ratio can be written as

$$\ell_n = \frac{\mathcal{CN}(\xi_n | \mathbf{0}, \Sigma)}{\mathcal{CN}(\xi_n | \mathbf{0}, \mathbf{R}_n + \Sigma)} = \frac{|\mathbf{R}_n + \Sigma|}{|\Sigma|} \exp(-\xi_n^H \Omega_n \xi_n). \quad (19)$$

Notice that (14) can be rewritten as $\theta_n^t = (1 + \frac{1-\epsilon_n}{\epsilon_n} \rho_n^t)^{-1}$.

With a large number of antennas, M_{tot} , a naive implementation of the AMP algorithm has two major drawbacks: 1) calculating the determinants and inverting the $M_{\text{tot}} \times M_{\text{tot}}$ matrices in (14), (15) and (16) can be computationally demanding; 2) sending the $L \times M_{\text{tot}}$ -dimensional matrix \mathbf{Y} requires high fronthaul capacity.

B. Covariance Structure in the AMP State Evolution

The received signal model in distributed MIMO, see (1), has a special property: the covariance matrices $\{\mathbf{R}_n\}$ are block-diagonal. In the following theorem, we show that during the state evolution in AMP, the states maintain the same block-diagonal structure during all iterations.

Theorem 1. *Assume that $\{\mathbf{R}_n\}$ have a block-diagonal structure: $\mathbf{R}_n = \text{bdiag}(\mathbf{R}_{1n}, \dots, \mathbf{R}_{Kn})$. By using the MMSE denoiser in (13), the state Σ^t in the state evolution (11) stays as a block-diagonal matrix with the same structure for each block, i.e., $\Sigma^t = \text{bdiag}(\Sigma_1^t, \dots, \Sigma_K^t)$, for all t .*

Proof. See Appendix A. \square

According to Theorem 1, the inversion of the $M_{\text{tot}} \times M_{\text{tot}}$ matrices in (15) and (16) can be performed by inverting their diagonal blocks, which are of dimension $M \times M$ ².

When the channel vector from device n to AP k is modeled by i.i.d. Rayleigh fading, the channel covariance matrix becomes $\tilde{\mathbf{R}}_{kn} = \beta_{kn} \mathbf{I}_M$. Correspondingly, the effective channel \mathbf{h}_n from device n to all APs has the distribution $\mathcal{CN}(\mathbf{0}, \mathbf{R}_n)$ with $\mathbf{R}_n = \text{bdiag}(\rho_{1n} \mathbf{I}_M, \dots, \rho_{Kn} \mathbf{I}_M)$. The following corollary can be viewed as a generalization of [2, Theorem 1] to the scenario of distributed MIMO.

Corollary 1. *Assume that $\{\mathbf{R}_n\}$ have the diagonal structure $\mathbf{R}_n = \text{bdiag}(\rho_{1n} \mathbf{I}, \dots, \rho_{Kn} \mathbf{I})$. By using the MMSE denoiser in (13), the state Σ^t stays as a scaled identity matrix for each diagonal block, i.e., $\Sigma^t = \text{bdiag}(\tau_1^t \mathbf{I}, \dots, \tau_K^t \mathbf{I})$, for all t .*

Proof. By setting the size of the diagonal blocks in Theorem 1 to one, we conclude that the state Σ^t stays as a diagonal matrix. Then, by using the symmetry, we conclude that the elements corresponding to the same AP are equal. \square

In the i.i.d. Rayleigh case, the calculations of all matrix inversions and determinants simplify to scalar operations.

C. Distributed Activity Detection

Since by Theorem 1, Σ and Ω_n are both block-diagonal, we can rewrite the likelihood-ratio in (19) as

$$\ell_n = \prod_{k \in \mathcal{K}} \underbrace{\frac{|\mathbf{R}_{kn} + \Sigma_k|}{|\Sigma_k|} \exp(-\xi_{kn}^H \Omega_{kn} \xi_{kn})}_{\triangleq \ell_{kn}}. \quad (20)$$

²For simplicity, we assume that all APs have the same number of antennas. The algorithm, however, can be easily modified to support arbitrary numbers of antennas.

Algorithm 1 distributed AMP (dAMP)

Input: $\Phi, \{\mathbf{Y}_k\}, \{\mathbf{R}_{kn}\}$

Initialize: $\mathbf{Z}_k^0 = \mathbf{Y}_k$, $\hat{\mathbf{x}}_{kn} = \mathbf{0}$, and $\Sigma_k^0 = \frac{1}{L} \mathbf{Y}_k^T \mathbf{Y}_k^*$, $\forall k, \forall n$

```

1: for each  $k \in \mathcal{K}$ , independently do
2:   for  $t = 0, 1, \dots$  do
3:     for each  $n \in \mathcal{N}_k^d$  do
4:        $\xi_{kn}^t = (\mathbf{Z}_k^t)^T \phi_n^* + \hat{\mathbf{x}}_{kn}^t$ 
5:        $\Psi_{kn}^t = \mathbf{R}_{kn} (\mathbf{R}_{kn} + \Sigma_k^t)^{-1}$ 
6:        $\Omega_{kn}^t = (\Sigma_k^t)^{-1} - (\mathbf{R}_{kn} + \Sigma_k^t)^{-1}$ 
7:        $\rho_{kn}^t = \frac{|\mathbf{R}_{kn} + \Sigma_k^t|}{|\Sigma_k^t|} \exp(-(\xi_{kn}^t)^H \Omega_{kn}^t \xi_{kn}^t)$ 
8:        $\theta_{kn}^t = (1 + \frac{1-\epsilon_n}{\epsilon_n} \rho_{kn}^t)^{-1}$ 
9:        $\hat{\mathbf{x}}_{kn}^t = \theta_{kn}^t \Psi_{kn}^t \xi_{kn}^t$ 
10:    end for
11:     $\mathbf{U}_k^t = \frac{1}{N} \sum_{n \in \mathcal{N}_k^d} \theta_{kn}^t \Psi_{kn}^t (\mathbf{I} + (1 - \theta_{kn}^t) \xi_{kn}^t (\xi_{kn}^t)^H \Omega_{kn}^t)$ 
12:     $\mathbf{Z}_k^{t+1} = \mathbf{Y}_k - \sum_{n \in \mathcal{N}_k^d} \phi_n (\hat{\mathbf{x}}_{kn}^t)^T + \frac{N}{L} \mathbf{Z}_k^t \mathbf{U}_k^t$ 
13:     $\Sigma_k^{t+1} = \frac{1}{L} (\mathbf{Z}_k^{t+1})^T (\mathbf{Z}_k^{t+1})^*$ 
14:  end for
15: end for

```

Equivalently, the LLR is

$$\log \ell_n = \sum_{k \in \mathcal{K}} \log \ell_{kn}, \quad (21)$$

where

$$\log \ell_{kn} = \log \frac{|\mathbf{R}_{kn} + \Sigma_k|}{|\Sigma_k|} - \xi_{kn}^H \Omega_{kn} \xi_{kn}. \quad (22)$$

Here, Σ_k and Ω_{kn} are the k -th diagonal blocks of Σ and Ω_n , respectively, and ξ_{kn} is the corresponding subvector of ξ_n . This means that the LLR $\log \ell_n$ can be written as the sum of $\{\log \ell_{kn}\}$, which can be interpreted as the *local* LLRs after *coherently* processing the received signals at each AP.

In the special case of i.i.d. Rayleigh fading, the LLR can be further simplified into

$$\log \ell_{kn} = M \log \left(1 + \frac{\rho_{kn}}{\tau_k} \right) - \frac{\rho_{kn} \|\xi_{kn}\|^2}{\tau_k (\rho_{kn} + \tau_k)}, \quad (23)$$

where the quantity ρ_{kn}/τ_k can be interpreted as the signal-to-noise ratio (SNR).

Inspired by the factorization in (20), we propose a distributed approach to activity detection in distributed MIMO. The procedure is as follows: each AP runs the AMP algorithm locally by using only the received signal \mathbf{Y}_k and sends the local LLR $\log \ell_{kn}$ to the aggregator. Then, the aggregator computes the LLR $\log \hat{\ell}_n = \sum_{k \in \mathcal{K}} \log \hat{\ell}_{kn}$ for activity detection.

D. Dynamic Cooperation Clustering

We assumed that each device was served by all APs. This configuration is not scalable in complexity and resource requirements as $N \rightarrow \infty$. Meanwhile, the AMP algorithm, or more generally, CS techniques, are known to work in the regime where the measurement size (pilot length) is larger than or equal to the support size (number of active devices).

To address these issues, we consider a dynamic cooperation clustering (DCC) framework, such that a device is served only by the APs with indices in the set $\mathcal{K}_n^d \subset \mathcal{K}$. Conversely, an

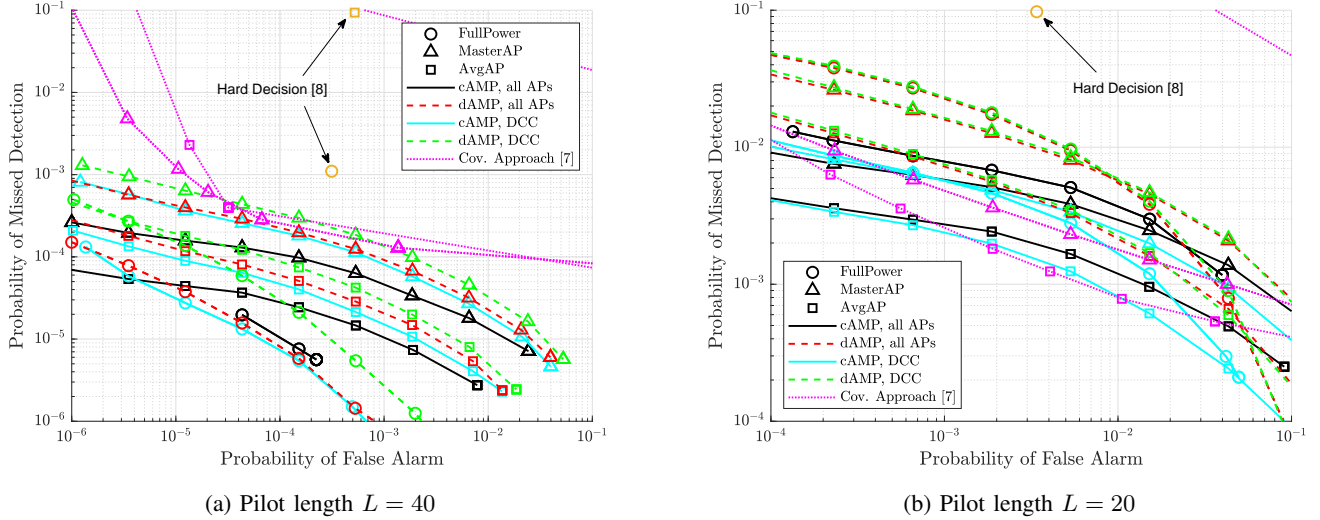


Fig. 1: Performance of the cAMP, dAMP, and baseline algorithms with different power allocation schemes.

AP only serves a subset of devices $\mathcal{N}_k^d = \{n \in \mathcal{N} : k \in \mathcal{K}_n^d\}$. There are two advantages of using the DCC framework: 1) the computational complexity is reduced; 2) the effective number of active devices served by an AP decreases.

Finally, by exploiting the DCC framework and our new findings about the MMSE denoiser, we propose a distributed AMP (dAMP) which is detailed in Algorithm 1. A centralized AMP (cAMP) is also developed in a similar way, while the step-wise details are omitted owing to space constraints. The key distinction in cAMP is that the denoiser for device n is designed using $\theta_n^t = \left(1 + \frac{1-\epsilon_n}{\epsilon_n} \prod_{k \in \mathcal{K}_n^d} \ell_{kn}^t\right)^{-1}$ by combining the local LLRs from all its serving APs in each iteration. These algorithms can be modified for other network structures. For example, multiple neighboring APs can coherently process the received signals. In this respect, cAMP (fully coherent) and dAMP (noncoherent) represent two extreme cases.

E. Complexity Analysis

The computational complexity of dAMP with correlated fading is dominated by the calculation of matrix inversions and determinants in steps 5-7 of Algorithm 1 with complexity $O(M^3)$. Therefore, the overall complexity is $O(KTNM^3)$. For the i.i.d. Rayleigh case, the complexity of matrix-vector multiplications in steps 4, 7, and 9 is $O(M^2)$, and the matrix multiplications in steps 12 and 13 have complexity $O(LM^2)$. Since we are interested in the regime where $L \ll N$, the overall complexity becomes $O(KTNM^2)$. Notice that dAMP can be distributed, and the processing per AP has complexity $O(TNM^2)$. Furthermore, by using the DCC framework, we can replace N by $\max_k |\mathcal{N}_k^d|$.

For comparison, the covariance-based method in [7] has overall complexity $O(TN(K_{\text{dom}}^3 + KL^2))$, where K_{dom} is the number of dominant APs; for the typical case $K_{\text{dom}} < L$, the complexity becomes $O(KTNL^2)$. Note, however, that method of [7] is developed for the i.i.d. Rayleigh case and while extensions are possible, they are likely to incur higher complexity. Since the number of antennas is typically small

	cAMP		dAMP		Cov. approach
	all APs	DCC	all APs	DCC	
$L = 40$	0.69	0.28	0.38	0.21	2.33
$L = 20$	0.70	0.29	0.37	0.21	1.34

TABLE I: Runtime comparison in seconds.

on an AP, we have $M < L$, and our algorithms have lower complexity than that of [7].

IV. SIMULATIONS

We consider a distributed MIMO system with $K = 20$ APs with $M = 3$ antennas each. A total of $N = 400$ devices are randomly dropped in a $2 \text{ km} \times 2 \text{ km}$ squared area with activity probability $\epsilon_n = 0.1, \forall n$. By using a wrap-around technique, we approximate an infinitely large network with 15 antennas and 10 active devices per square km. The pilots are random Gaussian sequences normalized to unit energy. The maximum transmit power is 23 dBm. The bandwidth is 1 MHz. The noise power spectral density is -169 dBm/Hz . The LSFC is generated by $-140.6 - 36.7 \log_{10}(d_n) + \Upsilon_i$ in dB, where d_n is the distance from device n to the AP in km, and Υ_n is the shadow fading effect distributed as $\mathcal{N}(0, \sigma_{\text{sf}}^2)$, with standard deviation $\sigma_{\text{sf}} = 4 \text{ dB}$. The small-scale fading is modeled by i.i.d. Rayleigh for each pair of AP and device. The LSFC threshold for power allocation is set to satisfy $p_{\text{max}} \beta_n^{\text{th}} = 6 \text{ dB}, \forall n$. For the DCC framework, we connect each device to the 10 APs with the largest LSFC.

The performances of cAMP and dAMP are examined in Fig. 1 with or without the DCC framework and with different power allocation schemes.³ The covariance-based approach in [7] (with 3 dominant APs) and the hard-decision-and-fusion based AMP method⁴ in [8] are used as baselines for

³Code available at <https://github.com/jiananbai/distributed-AMP>.

⁴Since [8] provided neither theoretical results nor algorithm details for the multi-antenna AP case, we use the expressions of probabilities of missed detection and false alarm in [2] to perform the decision fusion. Notice that this method uses a minimum-probability-of-error criterion and does not produce receiver operating characteristic (ROC) curves.

comparison. A runtime comparison is provided in Table I.⁵

The results for pilot length $L = 40$ are shown in Fig. 1a. The following observations can be made: (i) When the pilot length is larger than or equal to the average number of active devices, AMP outperforms the covariance-based approach in almost all configurations since our AMP algorithms can coherently process received signals from more APs. (ii) AMP works better with full power. We hypothesize that this is because of the macro-diversity in distributed MIMO: for each device there are almost always some APs to which the path gain is high. Thus, although using full power usually works poorly for activity detection in co-located MIMO, it can be an option in distributed MIMO where it is difficult to obtain an explicit objective for optimizing the power allocation. (iii) There is a performance gap between cAMP and dAMP due to the lack of coherent processing across different APs for dAMP.

In Fig. 1b, the results are reproduced for pilot length $L = 20$, which is not a working regime for AMP in the co-located case. We observe: 1) the performance loss of AMP is more significant than for the covariance-based approach since the AMP is inherently restricted to scenarios where $L \geq \sum a_n$, while the covariance-based approach has a better scaling law [5]; 2) AvgAP becomes a better power allocation scheme, potentially due to its better control of interference power under increased pilot contamination; 3) DCC performs better than using all APs, since an AP can ignore the devices with bad channel conditions; this is particularly helpful when L is small relative to the average number of active users.

V. CONCLUSION

We showed that for activity detection in distributed MIMO: 1) the AMP algorithm can be implemented in a distributed manner with an acceptable performance loss; 2) the AMP algorithm outperforms the covariance-based approach when the pilot length is larger than or equal to the average number of active devices, although this is not the case in co-located MIMO; 3) the problem of pilot correlation can be alleviated by using the DCC framework, when the pilot length is less than the average number of active devices.

APPENDIX A

We prove Theorem 1 by induction. First, when the covariance matrices $\{\mathbf{R}_n\}$ share a block-diagonal structure, the initial state Σ^0 in (12) has the same block-diagonal structure. Then, assuming that Σ^t stays in this structure, we show that Σ^{t+1} has the same structure.

Definition 1. (Partially Odd or Even Function) A function $f : \mathbb{R}^M \rightarrow \mathbb{R}$ is partially odd or even in indices $\mathcal{I} \subset \mathcal{M} = \{1, \dots, M\}$ if $f(\eta_{\mathcal{I}}(\mathbf{x})) = -f(\mathbf{x})$ or $f(\eta_{\mathcal{I}}(\mathbf{x})) = f(\mathbf{x})$, respectively. Here, $\eta_{\mathcal{I}}(\cdot)$ is an element-wise operator with $[\eta_{\mathcal{I}}(\mathbf{x})]_i$ equals to $-x_i$ for $i \in \mathcal{I}$, and x_i otherwise.

An arbitrary expectation term in the summand of the second term in the state evolution (11) can be written as

$$\begin{aligned} & \mathbb{E} \left[(\mathbf{g}(\mathbf{x} + \mathbf{v}, \Sigma) - \mathbf{x})(\mathbf{g}(\mathbf{x} + \mathbf{v}, \Sigma) - \mathbf{x})^H \right] \\ &= \mathbb{E} \left[\mathbf{g}(\mathbf{x} + \mathbf{v}, \Sigma) (\mathbf{g}(\mathbf{x} + \mathbf{v}, \Sigma))^H \right] + \mathbb{E} [\mathbf{x} \mathbf{x}^H] \\ & \quad - \mathbb{E} [\mathbf{g}(\mathbf{x} + \mathbf{v}, \Sigma) \mathbf{x}^H] - \mathbb{E} [\mathbf{x} (\mathbf{g}(\mathbf{x} + \mathbf{v}, \Sigma))^H]. \end{aligned} \quad (24)$$

According to (13), the first term equals

$$\underbrace{\Psi \mathbb{E} [\theta(\mathbf{x} + \mathbf{v})^2 (\mathbf{x} + \mathbf{v})(\mathbf{x} + \mathbf{v})^H] \Psi^H}_{\triangleq \mathbf{Q}}, \quad (25)$$

where $\theta(\cdot)$ is defined in (14). By denoting as $p_x(\mathbf{x})$ and $p_v(\mathbf{v})$ the density functions of \mathbf{x} and \mathbf{v} , respectively, the (i, j) -th element of \mathbf{Q} is given by

$$[\mathbf{Q}]_{i,j} = \int_{\mathbf{x}, \mathbf{v}} \underbrace{(x_i + v_i)(x_j + v_j)^* \theta(\mathbf{x} + \mathbf{v})^2 p_x(\mathbf{x}) p_v(\mathbf{v})}_{\triangleq f_{i,j}(\mathbf{x}, \mathbf{y})}. \quad (26)$$

Denote by \mathcal{M}_k the row (column) indices corresponding to the k -th diagonal block. Then $f_{i,j}(\mathbf{x}, \mathbf{y})$ is partially odd in \mathcal{M}_k if $i \in \mathcal{M}_k$ and $j \notin \mathcal{M}_k$, or $i \notin \mathcal{M}_k$ and $j \in \mathcal{M}_k$, and partially even in \mathcal{M}_k otherwise. That is, $[\mathbf{Q}]_{i,j} = 0$ if the indices i and j are not in the same diagonal block. This means that \mathbf{Q} is also block-diagonal with the same structure as $\{\mathbf{R}_n\}$. Then, the first term in (24), which equals to $\Psi \mathbf{Q} \Psi^H$, keeps the same block-diagonal structure.

By using similar arguments, one can show that the remaining terms have the same structure. We omit the details due to the limited space.

REFERENCES

- [1] H. Q. Ngo, A. Ashikhmin, H. Yang, E. G. Larsson, and T. L. Marzetta, "Cell-free massive MIMO versus small cells," *IEEE Trans. Wireless Commun.*, vol. 16, no. 3, pp. 1834–1850, 2017.
- [2] L. Liu and W. Yu, "Massive connectivity with massive MIMO—Part I: Device activity detection and channel estimation," *IEEE Trans. Signal Process.*, vol. 66, no. 11, pp. 2933–2946, 2018.
- [3] D. L. Donoho, A. Maleki, and A. Montanari, "Message-passing algorithms for compressed sensing," *Proceedings of the National Academy of Sciences*, vol. 106, no. 45, pp. 18914–18919, 2009.
- [4] M. Ke, Z. Gao, Y. Wu, X. Gao, and R. Schober, "Compressive sensing-based adaptive active user detection and channel estimation: Massive access meets massive MIMO," *IEEE Trans. Signal Process.*, vol. 68, pp. 764–779, 2020.
- [5] A. Fengler, S. Haghghatshoar, P. Jung, and G. Caire, "Non-Bayesian activity detection, large-scale fading coefficient estimation, and unsourced random access with a massive MIMO receiver," *IEEE Trans. Inf. Theory*, vol. 67, no. 5, pp. 2925–2951, 2021.
- [6] H. Djelouat, L. Marata, M. Leinonen, H. Alves, and M. Juntti, "User activity detection and channel estimation of spatially correlated channels via AMP in massive MTC," in *Proc. 55th Asilomar Conf. Signals, Syst., Comput.*, 2021, pp. 1200–1204.
- [7] U. K. Ganesan, E. Björnson, and E. G. Larsson, "Clustering-based activity detection algorithms for grant-free random access in cell-free massive MIMO," *IEEE Trans. Commun.*, vol. 69, no. 11, pp. 7520–7530, 2021.
- [8] M. Guo and M. C. Gursoy, "Joint activity detection and channel estimation in cell-free massive MIMO networks with massive connectivity," *IEEE Trans. on Commun.*, vol. 70, no. 1, pp. 317–331, 2022.
- [9] P. Han, R. Niu, M. Ren, and Y. C. Eldar, "Distributed approximate message passing for sparse signal recovery," in *IEEE Global Conference on Signal and Information Processing (GlobalSIP)*, 2014, pp. 497–501.
- [10] R. Hayakawa, A. Nakai, and K. Hayashi, "Distributed approximate message passing with summation propagation," in *Proc. IEEE Int. Conf. Acoust., Speech, Signal Process.*, 2018, pp. 4104–4108.

⁵The simulations were performed on an Intel Xeon Gold 6130 Processor.